SUPPORTING INFORMATION FOR

Unraveling the complexity of atmospheric brown carbon produced by smoldering boreal peat using size-exclusion chromatography with selective mobile phases

Ming Lyu,[1] Dan K. Thompson,[2#] Nianci Zhang,[1] Chad W. Cuss,[3ξ]
Cora J. Young,[4] and Sarah A. Styler[1,5*]

*Corresponding author. Email: stylers@mcmaster.ca. Phone: (780) 492-6659

[1] Department of Chemistry, University of Alberta, Edmonton, Alberta, Canada
[2] Natural Resources Canada - Northern Forestry Centre, Edmonton, Alberta, Canada
[3] Department of Renewable Resources, University of Alberta, Edmonton, Alberta, Canada
[4] Department of Chemistry, York University, Toronto, Ontario, Canada
[5] Department of Chemistry & Chemical Biology, McMaster University, Hamilton, Ontario, Canada

[#] Now at Natural Resources Canada - Great Lakes Forestry Centre, Sault Ste. Marie, Canada
[ξ] Now at School of Science and the Environment, Memorial University of Newfoundland (Grenfell Campus), Corner Brook, Newfoundland and Labrador, Canada

1 Supplementary text

2 Supplementary figures

S3 Single-wavelength absorption chromatograms (300 nm) for BrC and SRHA as a function of mobile phase phosphate buffer concentration (*i.e.*, ionic strength)
S4 Absorption density plots for PILS samples collected during/after peat combustion
S5 Absorption density plots for a particle-free PILS sample
S6 Absorption density plots for an ambient air PILS sample collected in the combustion laboratory
S7 SEC analysis of an aqueous extract of a simultaneously collected QFF $PM_{2.5}$ sample

3 Supplementary tables

S1 Molecular weight (MW) of SRHA, as estimated via SEC analysis using PSS calibration curves constructed under different mobile phase conditions
S2 SEC retention time reproducibility for acetone and SRHA

1 Supplementary text

1.1 Calibration curves of polystyrene sulfonate (PSS) standards as a function of mobile phase composition

To characterize our SEC column, we used PSS standards to construct calibration curves under a variety of mobile phase conditions (**Figure S1**). We used log-linear fits of these calibration data (*i.e.*, log MW of PSS standards versus retention volume; we excluded acetone from the fits, as we used it only as the marker for total permeation volume) to estimate the MW of SRHA, which we analyzed under the same conditions (**Table S1**). As discussed in the main text, the SRHA MW estimates thus obtained changed substantially as a function of mobile phase composition. Here, we discuss these changes in more detail.

The largest changes in estimated SRHA MW occurred when the mobile phase ionic strength was varied in the absence of organic modifiers: at 20 mM phosphate buffer, the estimated MW was ~3 kDa, whereas at 100 mM phosphate buffer, the estimated MW was >10 kDa. These results can be explained by differences in the three-dimensional structures of PSS and SRHA, which lead to different susceptibilities to electrostatic effects. Specifically, because PSS is a strong polyelectrolyte with a linear structure,[1] its elution behaviour is influenced both by ionic exclusion resulting from repulsion between its negatively-charged sulfonate groups and the negatively-charged column matrix and by chain expansion/coiling resulting from changes in the magnitude of ionic repulsion between neighbouring sulfonate groups.[1,2] By contrast, because SRHA has a more branched and cross-linked structure,[3] and contains only weakly acidic functional groups (*e.g.*, carboxyl groups),[4] it is less subject to ionic exclusion and its conformation

is less influenced by intramolecular electrostatic effects. These structural differences lead to underestimation of SRHA MW at lower ionic strengths, due to the earlier elution of expanded and ionically excluded PSS standards, and overestimation at higher ionic strengths, due to the later elution of coiled PSS standards.

An additional potential explanation for these variations in estimated SRHA MW involves hydrophobic interactions with the column matrix, which we expect to be significant at elevated ionic strengths.[5] Indeed, in the presence of 100 mM phosphate buffer, addition of 10% MeOH led to a substantial decrease in the retention times of PSS standards. Because this addition had only a negligible effect on overall mobile phase ionic strength, these results suggest that the elution behaviour of PSS standards at high mobile phase ionic strengths is influenced substantially by hydrophobic interactions. By contrast, SRHA exhibited a negligible shift in retention time upon addition of 10% MeOH, which suggests that hydrophobic interactions are less important for this analyte and/or that this concentration of organic modifier was insufficient to mitigate any hydrophobic interactions that do exist. As a result of these different responses to organic modifier addition, the estimated SRHA MW was much lower in the presence of 10% MeOH (~4 kDa) than in its absence (~11 kDa).

At lower ionic strengths, the effects of organic modifier addition are less pronounced: in the presence of 20 mM phosphate buffer, the estimated MW decreased from ~3 kDa at 0% ACN to <1 kDa at 50% ACN. In the presence of ACN (25%), both PSS and SRHA eluted earlier than when phosphate buffer alone was used as mobile phase; at higher ACN contents, however, the retention time of SRHA remained relatively constant, whereas the PSS eluted even earlier. We suggest that these observations reflect the influence of both hydrophobic and electrostatic secondary interactions: although the

addition of ACN suppresses hydrophobic interactions between the analytes and the column matrix, it also lowers the overall mobile phase ionic strength; as a result, the elution behaviour of these analytes at higher ACN contents is mainly determined by electrostatic effects. Because, as discussed previously, PSS is more susceptible than SRHA to ionic exclusion and intramolecular electrostatic effects, it eluted progressively earlier with increasing ACN content, which ultimately resulted in lower estimated SRHA MW values. We note that the addition of ACN also resulted in a reduction in the total permeation volume, as reflected by the earlier elution of acetone (see **Table S1**); however, if this were the only factor underlying the earlier elution of PSS and SRHA, they would have been influenced identically, which was not the case.

1.2 Quality control experiments

Under our experimental conditions, solid residue rapidly built up on the quartz impactor plate; in order to minimize transfer of this insoluble material to the collection vials,[6] we disassembled and cleaned the impactor plate and the stainless steel wick after every one or two experiments, depending on the smoke intensity. To exclude this and other potential PILS-specific sampling artifacts, we analyzed three additional sample types. First, to determine the importance of sample-to-sample carryover of sparingly soluble light-absorbing material, we analyzed wash flow samples collected before, during, and after combustion. Second, to assess the contribution of soluble gases to the observed light absorption profile, we conducted one experiment in which the PILS sample inlet was equipped with a HEPA filter (Brechtel). Finally, to assess the magnitude of absorbance contributions from background $PM_{2.5}$ in the combustion facility, we sampled ambient laboratory air prior to commencing each day's experiments. As shown

and discussed in **Figures S4–S6** and their associated captions, we do not expect our results to be affected by these considerations.

1.3 Collection and preparation of quartz fiber filter (QFF) $PM_{2.5}$ samples

To ensure that our observations reflected intrinsic BrC properties (*i.e.*, were not specific to PILS-collected samples), we also analyzed aqueous extracts of $PM_{2.5}$ samples collected simultaneously using quartz fiber filters (QFF). Here, combustion PM was sampled through a cyclone (5 LPM for $PM_{2.5}$; SCC 1.829, BGI), which was placed at the same height as the PILS inlet; sample collection began at peat ignition and continued for 5 min. The $PM_{2.5}$ flow was separated into two streams, each of which was controlled by a mass flow controller set to a flow rate of 2.5 L min^{-1}; a laboratory vacuum downstream of the mass flow controllers maintained the sampling flow. $PM_{2.5}$ was collected in one of the streams using a polycarbonate in-line filter holder (47 mm, Pall Laboratory) equipped with a 47 mm prebaked (500°C, 4 h) quartz fiber disc (Pallflex Tissuquartz Filters, Pall Laboratory). QFF samples were wrapped in pre-baked (500°C, 4 h) aluminum foil immediately after collection and refrigerated at 4°C until analysis.

Immediately prior to extraction, QFF samples were subsampled using a 10 mm stainless steel arc punch (McMaster-Carr); for the sample studied here, 4 sub-punches were used for extraction. Sub-punches were placed in a 4 mL amber glass vial (Thermo Scientific) to which 1 mL deionized water was added. Vials were closed with acid-washed, PTFE-lined caps (Thermo Scientific), sealed with Parafilm™ , and placed on a laboratory shaker (multi-platform shaker, Fisher Scientific) for 1 h. Extracts were filtered with PTFE syringe filters (0.2 μm, 13mm, Fisherbrand Basix) prior to SEC-PDA analysis.

As shown in **Figure S7a**, as was the case for the PILS BrC samples, the BrC chromophores in the QFF extracts fall into two fractions: a high-MW fraction with featureless absorption, and a low-MW fraction with a structured absorption profile in the UV region. Again, as was the case for the PILS BrC samples, the fraction of the total absorption contributed by the low-MW fraction increased with increasing mobile phase ACN content (**Figure S7b**). These results support our conclusion that fresh BrC from boreal peat combustion is made up of chromophores with a wide range of sizes and polarities, and in particular show that the results discussed in the main text are not specific to the PILS sample collection system but rather reflect intrinsic properties of the emitted BrC.

1.4 Integration procedure for SEC absorption density plots

As shown in **Figure 2** of the main text, the absorption density plots of our BrC sample change substantially with changes in mobile phase composition. To quantitatively compare the BrC absorption profiles observed under different mobile phase conditions, and to better understand how the size distribution of BrC chromophores changes as a function of organic modifier identity, we determined the total absorbance for the high- and low-MW fractions described in **Section 3.2.2** of the main text as follows. For the high-MW fraction, which exhibited featureless, tailing absorption, we integrated from 220 nm to 500 nm across its elution range. For the low-MW fraction, which eluted toward the total permeation volume and exhibited structured absorption, we integrated from 220 nm to the wavelength at which the total absorption across the elution range was less than 5% of its maximum value. To standardize contributions from background signal noise, we integrated from the time associated with the end of the high-MW

fraction to the time at which the total absorption (220–500 nm) was less than 5% of its maximum value.

1.6 References

(1) Sen, A. K.; Roy, S.; Juvekar, V. A. *Polymer International* **2007**, *56* (2), 167–174.
(2) Pavlov, G. M.; Gubarev, A. S.; Gavrilova, I. I.; Panarin, E. F. *Polym. Sci. Ser. A* **2011**, *53* (11), 1003–1011.
(3) Piccolo, A. In *Advances in Agronomy*; Academic Press, 2002; Vol. 75, pp 57–134.
(4) Prado, A. G. S.; Pertusatti, J.; Nunes, A. R. *Journal of the Brazilian Chemical Society* **2011**, *22* (8), 1478–1483.
(5) Hongve, D.; Baann, J.; Becher, G.; Lømo, S. *Environment International* **1996**, *22* (5), 489–494.
(6) Wonaschuetz, A.; Haller, T.; Sommer, E.; Witek, L.; Grothe, H.; Hitzenberger, R. *Aerosol Science and Technology* **2019**, *53* (1), 21–28.

Figure S1

Calibration curves of polystyrene sulfonate (PSS) standards as a function of mobile phase composition (mixture of buffer and organic modifier); here, buffer = 20–150 mM phosphate buffer (pH 6.8) and organic modifier = 0–50% (v/v) MeOH or ACN. Acetone retention times are also shown, but were not used for calibration.

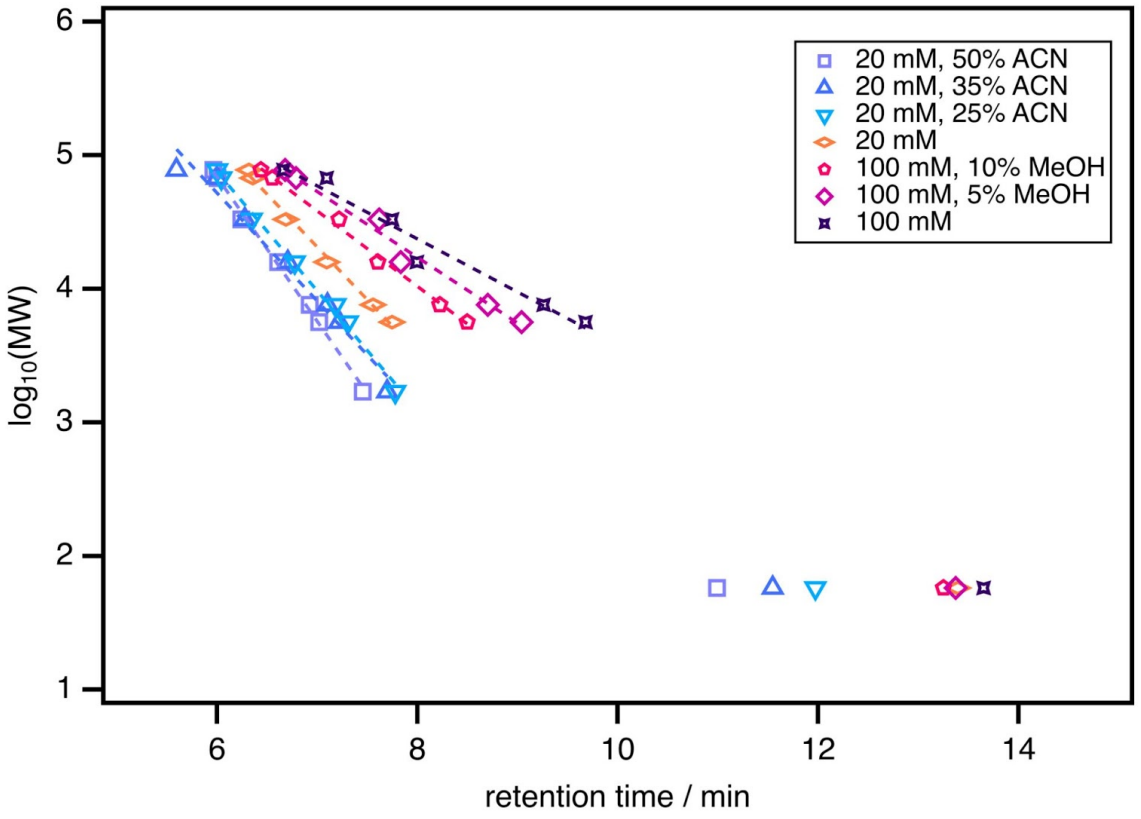

Figure S2

Absorption density plots for Suwannee River humic acid (SRHA) as a function of mobile phase organic modifier (ACN) content (v/v): a) 25%, b) 50%, c) 60%, d) 70%. In all cases, the remainder of the mobile phase was 20 mM phosphate buffer (pH 6.8).

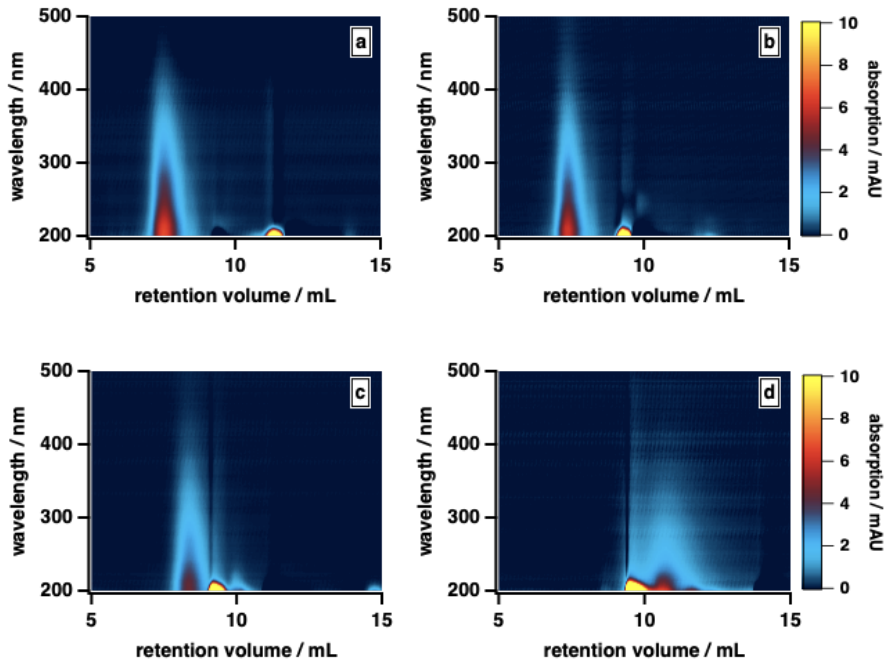

Figure S3

Single-wavelength absorption chromatograms (300 nm) for fresh peat BrC (—), SRHA (—), and acetone (—) as a function of mobile phase phosphate buffer concentration (*i.e.*, ionic strength). Mobile phases were prepared using three concentrations of phosphate buffer (pH 6.8): a) 10 mM, b) 20 mM, c) 40 mM. In all cases, the mobile phase composition (v/v) was 50% phosphate buffer, 25% MeOH, and 25% ACN.

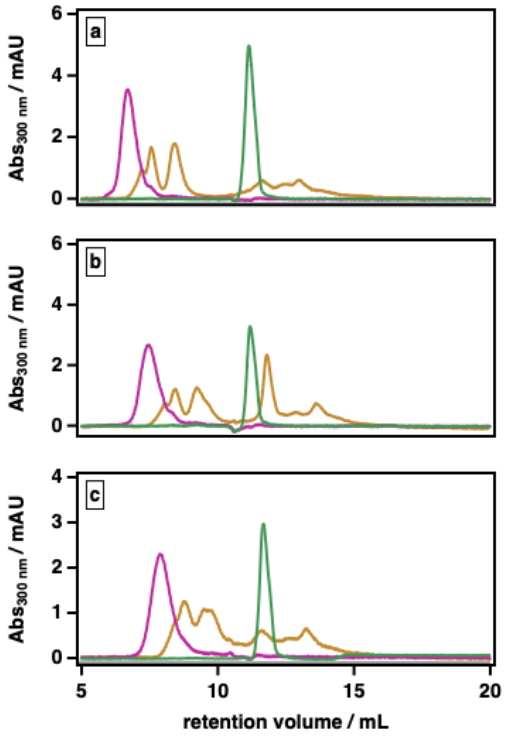

Figure S4

Absorption density plots of PILS samples collected during/after peat combustion. During the sampling process, solid residue gradually accumulated on the PILS impactor plate and stainless steel wick. To minimize transfer of this material to the PILS sampling vials, we thoroughly cleaned the impactor plate and stainless steel wick after every one or two combustion experiments. To quantify sample-to-sample carryover of insoluble absorbing material from the PILS impactor plate, we collected samples for a total of ~35 min (10 vials × 3.5 minutes per vial) after peat ignition for each combustion experiment. Here, we show results for PILS wash fluids collected at 0–3.5 min (W1), 3.5–7.0 min (W2), 10.5–14.0 min (W4), and 24.5–28 min (W8); "W "identifies the combustion experiment, and W1 is the sample discussed at length in the main text. These samples were analyzed under two organic modifier conditions: (a) 25% MeOH/25% ACN (v/v), (b) 40% MeOH/10% ACN (v/v). In both cases, the remainder of the mobile phase was 20 mM phosphate buffer (pH 6.8). As illustrated here, levels of BrC in the combustion facility were significantly reduced by 7 min after peat ignition; after an additional 7 min, the absorption intensity plot of the PILS wash fluid resembled that of blank wash fluid (DI water; see **Figure S4**). Given these results, we conclude that carryover of insoluble residues built up on the PILS impactor plate and wick did not lead to positive biases in measured absorption profiles for subsequent experiments.

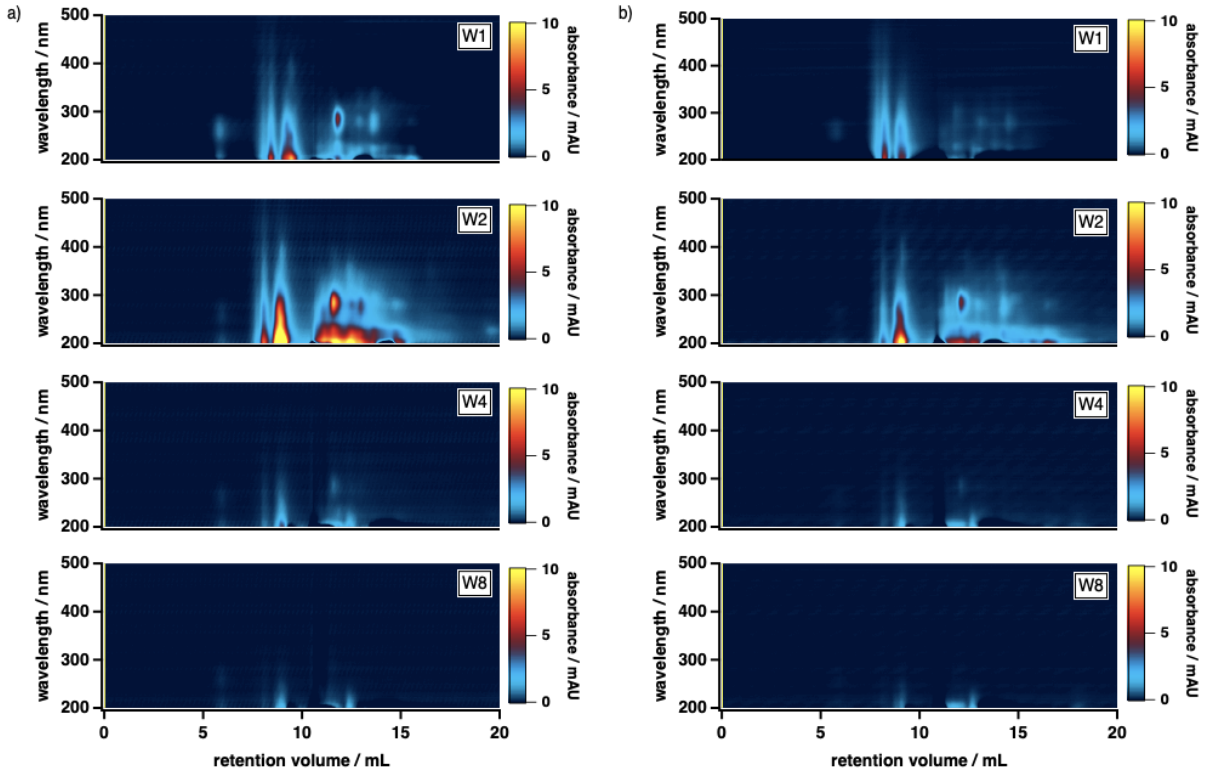

Figure S5

Absorption density plots for a particle-free PILS sample.
Biomass burning emits both particle- and gas-phase products. To determine whether our results were influenced by co-emitted gaseous species, we performed a control experiment in which a HEPA filter was attached to the PILS sampling inlet for the duration of peat combustion. Here, we burned the 10–15 cm subfraction of a peat sample collected at the same location as the sample discussed in the main text. The absorption density plots for the particle-free PILS sample (HEPA sample) were compared to those for a blank PILS wash fluid sample (DI water) under two organic modifier conditions: (a) 40% MeOH/10% ACN (v/v), (b) 25% MeOH/25% ACN (v/v). In both cases, the remainder of the mobile phase was 20 mM phosphate buffer (pH 6.8). As shown here, the absorption density plots for the HEPA sample are quite similar to those for the DI water sample, which implies that light-absorbing interferences from gas-phase emissions are largely eliminated by the VOC denuder applied to the PILS sampling inlet during the combustion experiments performed in this study.

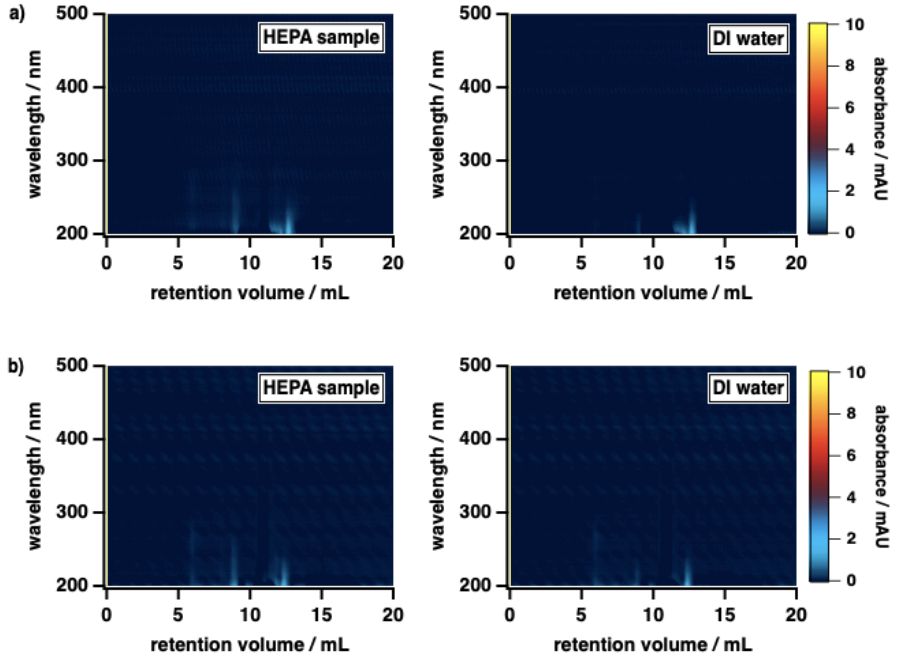

Figure S6

Absorption density plots for an ambient air PILS sample collected in the combustion laboratory.

To assess the magnitude of absorbance contributions from background $PM_{2.5}$ in the combustion facility, we sampled ambient laboratory air prior to commencing each day's experiments. Background sampling was conducted for ~18 min; here, we show results for 0–3.5 min (B31) and 14.0–17.5 min (B35) of the ambient air sampling process. These samples were analyzed under two organic modifier conditions: (a) 40% MeOH/10% ACN (v/v), (b) 25% MeOH/25% ACN (v/v). In both cases, the remainder of the mobile phase was 20 mM phosphate buffer (pH 6.8). Using these results, we estimate that the ambient background absorbance accounts for <7% of the total sample absorbance (here, the ambient background and sample absorption density plots were integrated over the same time and wavelength ranges), and conclude that interfering absorption from background $PM_{2.5}$ in the ambient laboratory air is negligible in this study.

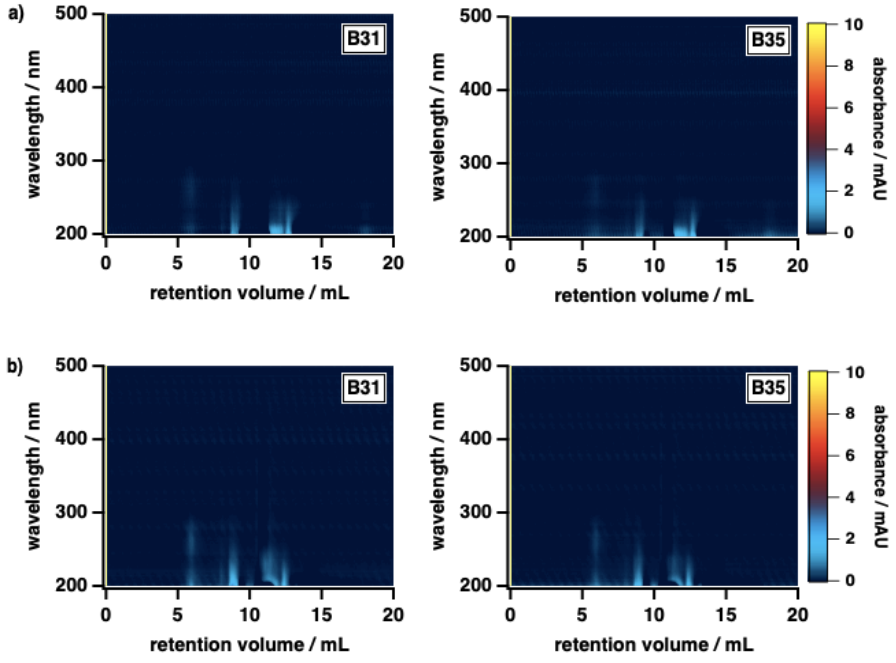

Figure S7

SEC analysis of an aqueous extract of a simultaneously collected QFF $PM_{2.5}$ sample. To verify that the results we describe in the main text were not PILS-specific, we also analyzed an aqueous extract of a simultaneously collected QFF $PM_{2.5}$ sample. Here, we present a) absorption density plots and b) absorption contributed by high-MW and low-MW BrC fractions for this extract under each of the following mobile phase organic modifier conditions: i) 50% MeOH / 0% ACN (v/v), ii) 40% MeOH / 10% ACN (v/v), iii) 25% MeOH / 25% ACN (v/v), iv) 0% MeOH / 50% ACN (v/v). In all cases, the remainder of the mobile phase was 20 mM phosphate buffer (pH 6.8). The results shown in **Figure S7b** were calculated using the integration procedure described in **Section 1.3** of this document.

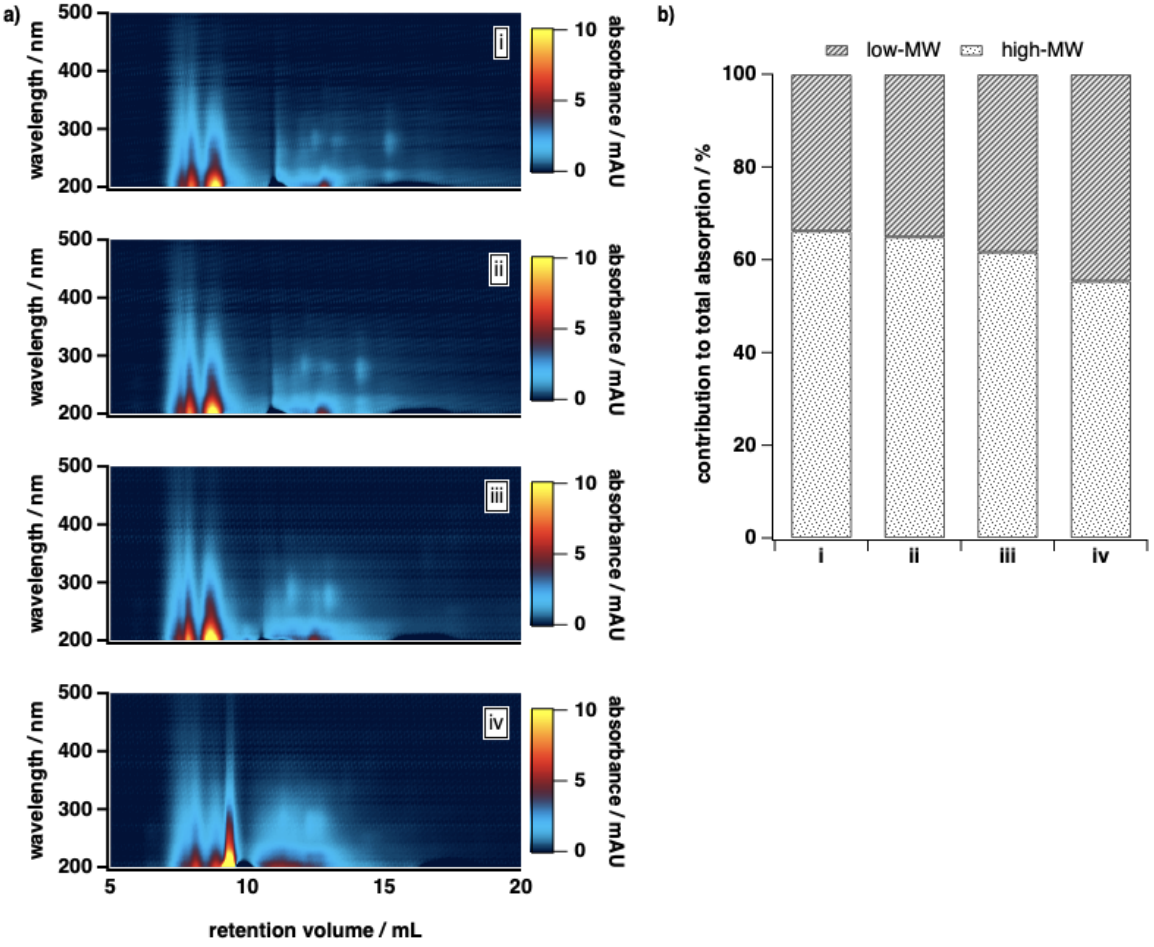

Table S1

Molecular weight (MW) of SRHA, as estimated via SEC analysis using PSS calibration curves constructed under different mobile phase conditions.

Mobile phase composition (PB = phosphate buffer, pH 6.8)	Vt (mL) (acetone)	PSS (5580 Da) retention time (min)	Equation of calibration curve	SRHA	
				Retention time (min)	Estimated MW (Da)
100% PB (20 mM)	13.4	7.746	y = -0.7745x + 9.7274	8.135	2672
75% PB (20 mM), 25% ACN	12.0	7.303	y = -0.8922x + 10.229	7.796	1876
65% PB (20 mM), 35% ACN	11.6	7.220	y = -0.9104x + 10.292	7.770	1652
50% PB (20 mM), 50% ACN	11.0	7.020	y = -1.0788x + 11.308	7.721	951
100% PB (100 mM)	13.7	9.679	y = -0.4056x + 7.6266	8.894	10451
95% PB (100 mM), 5% MeOH	13.4	9.041	y = -0.4944x + 8.1914	8.859	6479
90% PB (100 mM), 10% MeOH	13.3	8.498	y = -0.5746x + 8.6156	8.811	3571

Table S2

SEC retention time reproducibility for acetone and SRHA.
As shown here, at a given mobile phase composition ((v/v), 50% organic modifier and 50% phosphate buffer at varying concentrations), and volumetric flow rate (for clarity, each operating condition is shown in a different colour), the retention time of both acetone and SRHA showed a high level of reproducibility over multiple injections. The variation in retention time for these analytes is less than 3% for this system.

Date of analysis (all 2019)	Retention time (min)				Mobile phase composition	Flow rate (mL min^{-1})
	acetone		SRHA			
02-May	10.978	10.981	6.865	6.876	50%ACN, 10mM	1.000
03-May	14.576	14.579	9.248	9.252	50%MeOH, 20mM	0.800
06-May	11.092	11.059	6.426	6.419	50%ACN, 5mM	1.000
09-May	10.988	10.988	6.352	6.366	50%ACN, 5mM	1.000
10-May	11.169	11.169	6.701	6.707	25%MeOH/25%ACN, 10mM	1.000
12-May	11.195	11.184	7.871	7.882	25%MeOH/25%ACN, 40mM	1.000
30-May			9.122	9.126	40%MeOH/10%ACN, 20mM	0.800
31-May	14.33	14.342	9.164	9.163	40%MeOH/10%ACN, 20mM	0.800
12-Jun	14.277	14.276	9.209	9.214	40%MeOH/10%ACN, 20mM	0.800
18-Jun	14.302	14.288			40%MeOH/10%ACN, 20mM	0.800
26-Jun	14.266	14.264	9.094	9.093	40%MeOH/10%ACN, 20mM	0.800
29-Jun	11.096	11.098	7.237	7.242	25%MeOH/25%ACN, 20mM	1.000
30-Jun	14.283				40%MeOH/10%ACN, 20mM	0.800
03-Oct	11.125	11.126			25%MeOH/25%ACN, 20mM	1.000
04-Oct	14.385				40%MeOH/10%ACN, 20mM	0.800
07-Oct	11.131	11.148			25%MeOH/25%ACN, 20mM	1.000
08-Oct	14.372	14.385			40%MeOH/10%ACN, 20mM	0.800
09-Oct	14.356	14.366	9.087	9.133	40%MeOH/10%ACN, 20mM	0.800
11-Oct	14.272	14.292	9.034	9.097	40%MeOH/10%ACN, 20mM	0.800
12-Oct	11.142	11.151	7.199		25%MeOH/25%ACN, 20mM	1.000
15-Oct	10.985	10.991	7.459	7.488	50%ACN, 20mM	1.000
16-Oct	14.268	14.285	8.969		40%MeOH/10%ACN, 20mM	0.800
05-Nov					40%MeOH/10%ACN, 20mM	0.800
06-Nov	14.297	14.261	8.941		40%MeOH/10%ACN, 20mM	0.800
07-Nov	10.954	10.962	7.403		50%ACN, 20mM	1.000
14-Nov	14.227		8.925		50%MeOH, 20mM	0.800
15-Nov	10.942	10.947	7.4	7.348	50%ACN, 20mM	1.000
18-Nov	14.264	14.276	8.95		40%MeOH/10%ACN, 20mM	0.800
19-Nov	10.932	10.951	7.367		50%ACN, 20mM	1.000